

## Article

# Mechanical and Fracture Properties of Air-Entrained FRC Containing Zeolitic Tuff

Zinovi Blikharskyy <sup>1</sup>, Taras Markiv <sup>2</sup>, Yurii Turba <sup>3</sup>, Oleksii Hunyak <sup>3</sup>, Yaroslav Blikharskyy <sup>3</sup>  
and Jacek Selejdak <sup>1,\*</sup>

<sup>1</sup> Faculty of Civil Engineering, Czestochowa University of Technology, 69 Street Dabrowskiego, 42-201 Czestochowa, Poland; zinovi.blikharskyy@pcz.pl

<sup>2</sup> Department of Building Production, Institute of Civil Engineering and Building Systems, Lviv Polytechnic National University, Karpinskoho Street 6, 79013 Lviv, Ukraine; taras.y.markiv@lpnu.ua

<sup>3</sup> Department of Highways and Bridges, Institute of Civil Engineering and Building Systems, Lviv Polytechnic National University, Karpinskoho Street 6, 79013 Lviv, Ukraine; yurii.v.turba@lpnu.ua (Y.T.); oleksii.m.guniak@lpnu.ua (O.H.); yaroslav.z.blikharskyy@lpnu.ua (Y.B.)

\* Correspondence: jacek.selejdak@pcz.pl

**Abstract:** This study aimed to evaluate the influence of zeolitic tuff, an air-entraining agent, and different types of fibers on the compressive strength and fracture parameters of concrete with increased strength. Notched beams were tested in three-point bending to determine the fracture parameters of concrete. It was established that the partial replacement of Portland cement (10% by mass) with zeolitic tuff, the addition of an air-entraining agent and different types of fibers resulted in the improvement both of the compressive strength (by 3.7% after 28 days of hardening) and fracture properties of concrete (namely, the fracture energy by 35.1% and characteristic length by 61.5%) compared to the reference concrete. The beneficial effects of the air-entraining agent and the mechanisms through which it enhances the properties of concrete by incorporating zeolitic tuff and various types of fibers were explained. It has been demonstrated that the appropriate selection and optimization of various technological factors enable the production of economically effective, high-quality concrete with a 10% lower cement content. As a result, this leads to reduced CO<sub>2</sub> emissions, aligning with a sustainable development strategy.

**Keywords:** air-entraining agent; concrete; fracture parameters; polypropylene fiber; strength



**Citation:** Blikharskyy, Z.; Markiv, T.; Turba, Y.; Hunyak, O.; Blikharskyy, Y.; Selejdak, J. Mechanical and Fracture Properties of Air-Entrained FRC Containing Zeolitic Tuff. *Appl. Sci.* **2023**, *13*, 9164. <https://doi.org/10.3390/app13169164>

Academic Editors: Tanvir Qureshi and Alessandro Arrigoni

Received: 7 July 2023

Revised: 8 August 2023

Accepted: 9 August 2023

Published: 11 August 2023



**Copyright:** © 2023 by the authors. Licensee MDPI, Basel, Switzerland. This article is an open access article distributed under the terms and conditions of the Creative Commons Attribution (CC BY) license (<https://creativecommons.org/licenses/by/4.0/>).

## 1. Introduction

During the last few decades, most countries have intensified their efforts to mitigate the adverse effects of the construction industry on the environment. From this point of view, developing and implementing effective technological solutions to produce concrete with improved performance parameters, especially fracture properties, is essential. The rational approach to properly selecting concrete constituents results in producing more durable materials and, in addition to environmental benefits, reducing investment costs. This corresponds to the requirements of sustainable construction. With the implementation of standards from the ISO 14000 family, the awareness of the Life Cycle Assessment (LCA) methodology has grown globally. This methodology serves as an assessment tool that yields consistent analytical outcomes, addressing various environmental issues [1].

Supplementary cementitious materials (SCMs), especially aluminosilicates (fly ash, zeolitic tuff, silica fume, etc.), offer numerous advantages to the transportation infrastructure and construction sector [2–4]. These materials are highly beneficial due to their availability, cost-effectiveness (especially when easily accessible), long-term mechanical properties, and ability to enhance durability [5,6]. Of particular interest is zeolitic tuff, which exhibits significant pozzolanic activity [7,8]. Abundant mineable zeolite deposits are found across numerous countries around the world. The yearly production of natural

zeolites has remained relatively stable for the past decade, with an approximate output of 3 million tons. The use of zeolitic tuff in concrete has been proven to enhance its durability significantly [9,10], along with its mechanical [11] and mass transport [12] properties. Previous studies [13,14] have demonstrated that replacing 10% by mass of cement with natural zeolite and using chemical admixtures leads to enhanced concrete properties and improved durability. For industrial and civil construction, it is crucial to find new additives to concrete that would satisfy operational parameters [15–21].

Nagrockiene et al. [22] studied modified zeolite's influence on the freeze–thaw and de-icing salt resistance of hardened cement paste; their results showed a significant improvement in density, strength, and frost resistance as well as resistance to the adverse effects of salts. Study [23] found that the frost resistance of zeolite-containing concrete exhibits a slightly lower performance than control concrete during the initial phase of freeze–thaw cycles. As the cycles progress, the frost resistance of zeolite-containing concrete significantly surpasses that of conventional concrete, which is related to the internal curing effect. However, the above-mentioned studies did not study the joint effect of the use of both zeolite and air-entraining agent.

The water absorption and freeze–thaw resistance of hardened concrete are essential parameters for bridge and pavement applications. According to Pleau et al. [24], it is predominantly influenced by factors such as the size, type, and distribution of pores and capillaries in concrete. Closed and tiny pores in such a structure are not entirely saturated with water, resulting in what is known as reserve pores. During freezing conditions, water may migrate towards these reserve pores, creating voids that accommodate ice expansion. Air-entraining admixtures proved to be a reliable method to improve fresh-concrete properties [25] and hardened-concrete performance, especially in a freeze–thaw environment [26]. However, there is a lack of studies regarding the influence of entrained air on the fracture parameters of concrete.

It is well known that concrete failure involves the formation and propagation of cracks: it exhibits a quasi-brittle behavior, combining characteristics of both brittleness and elastic-plasticity [27]. As concrete for infrastructure applications requires lower  $w/c$  ratios ( $<0.45$ ) to withstand aggressive exposure, it is more brittle than conventional concrete with  $w/c > 0.5$ . To predict and mitigate cracking in cement-based structures, approaches such as linear elastic fracture mechanics (LEFM) and fracture energy methods have proven effective [28]. The fundamental fracture properties of concrete, including the critical stress intensity factor, fracture energy, and characteristic length, can be determined using simple three-point bend notched beam specimens.

Previous tests [29] revealed that incorporating 10 wt.% zeolite and 5 wt.% limestone, along with chemical admixtures, demonstrated an increase in fracture properties. The authors suggested that this can be attributed to the consolidation of the concrete microstructure through the reaction between active silica in zeolite and calcium hydroxide, leading to the formation of larger quantities of calcium hydrosilicates. Furthermore, the absorption modification of hydrated products with chemical admixtures contributes to a higher strength and improved fracture properties in the modified concretes.

A common method to enhance concrete fracture properties is to incorporate polypropylene (PP) fibers of varying shapes, lengths, and characteristics into concrete at specific volumes [30]. The authors of [31] tested the compressive strength, flexural strength, and mid-span deflection of fiber-reinforced engineered cementitious composites blended with silica fume and zeolite. It was found that despite a low zeolite dosage (3 wt.%), it provided a better performance in combination with PP fibers in a sulfate environment, as evidenced by the significant increases in the studied parameters. Another experimental study [32] discussed the properties of an eco-friendly fiber-reinforced self-consolidated concrete with 10 wt.% zeolite. The authors established that samples with 0.50 to 0.75 vol.% of polyolefin fibers showed the highest compressive and tensile strength.

A previously conducted study [33] investigated the impact of PP fibers' addition on concrete's physical and mechanical properties. The experimental findings demonstrated

that incorporating PP fibers significantly enhanced the compressive and flexural strength as well as fracture energy. It was shown that the optimal combination of 0.675 and 3.5 kg/m<sup>3</sup> of micro- and macro-PP fibers, respectively, can synergistically increase the fracture parameters, benefiting both the pre-peak and post-peak stages.

Although the influence of each individual technological factor (content of zeolitic tuff, volume of entrained air, and dosage of fibers) has been sufficiently studied, there is limited information in the scientific literature regarding their combined effect. In this study, a work-of-fracture method is applied to assess the effect of the optimal combination of zeolitic tuff, two types of fibers, and an air-entraining agent on the performance of concrete under load.

## 2. Materials and Methods

Portland cement CEM II/A-S 52.5N was used in the research. The properties of the cement were determined according to [34–36]. The obtained results are shown in Table 1.

**Table 1.** Properties of the cement.

Specific Surface, m <sup>2</sup> /kg	Residue on Sieve 008, %	Water Demand, %	Setting Time, min		Compressive Strength, MPa	
			Initial	Final	2 Days	28 Days
350	2.6	29.0	140	230	27.1	54.2

The chemical compositions of Portland cement and zeolitic tuff (from Sokyrnytsia, Ukraine) were determined using an X-ray spectrometer ARL 9800 XP (Thermo Fisher Scientific, Waltham, MA, USA) and are shown in Table 2. The clinoptilolite content in zeolite was 68%.

**Table 2.** Chemical composition of cement and zeolitic tuff.

Material		CEM II/A-S 52.5N	Natural Zeolite
Chemical composition, %	SiO <sub>2</sub>	22.96	77.64
	Al <sub>2</sub> O <sub>3</sub>	4.85	13.04
	Fe <sub>2</sub> O <sub>3</sub>	3.59	2.90
	CaO	60.20	4.77
	MgO	2.04	1.60
	SO <sub>3</sub>	2.40	0.05
	LOI	3.96	-

The properties of aggregates were tested according to [37,38], and the obtained results are reported in Table 3. The water absorption for crushed granite aggregates was 0.4%.

**Table 3.** Properties of aggregates.

Aggregate Type	Density [g/cm <sup>3</sup> ]	Bulk Density [kg/m <sup>3</sup> ]	Voidage [%]	Dust and Clay Particles [%]	Fineness Modulus
Fine (quartz sand)	2.63	1502	42.9	0.2	1.6
Fine (crushed granite sand, 0.63–2 mm)	2.66	1464	45.0	0.6	-
Coarse (granite gravel, 5–10 mm)	2.66	1428	46.3	0.2	-
Coarse (granite gravel, 10–20 mm)	2.66	1465	44.9	0.5	-

Grading curves for the aggregates are given in Figure 1.

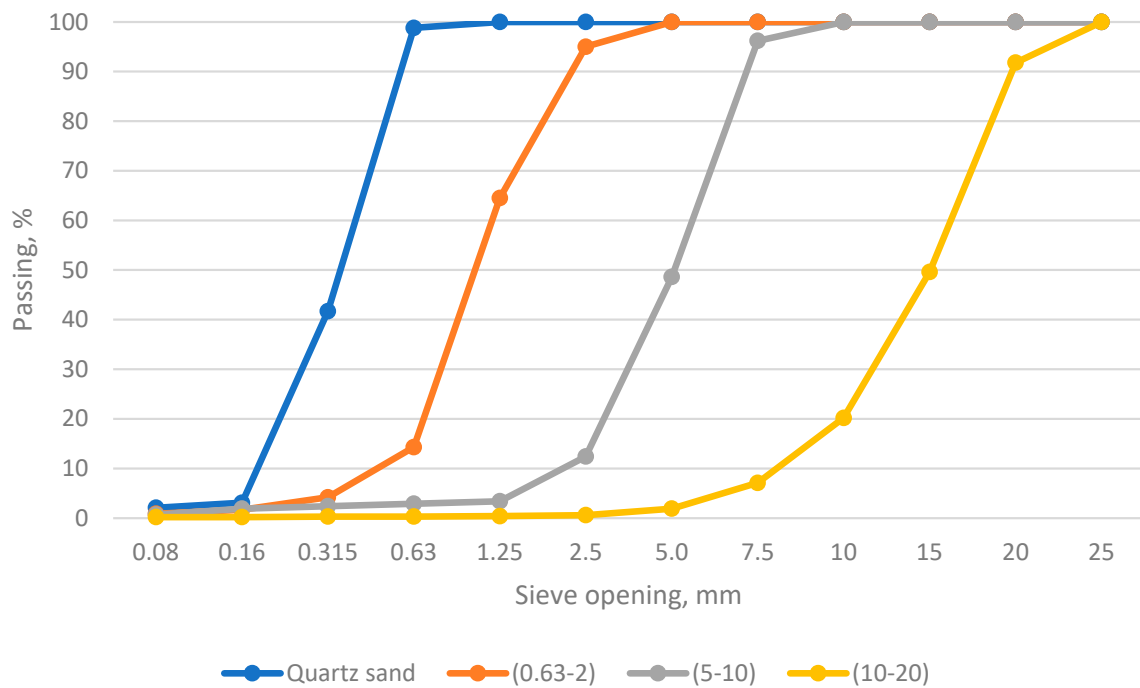


Figure 1. Grading curves for fine and coarse aggregates.

A commercially available polycarboxylate-based superplasticizer with a specific gravity of 1.05 and solid content of 30% and an air-entraining agent with a specific gravity of 1.02 and solid content of 2.5% were used in this study.

Polypropylene (PP) microfibers and fibers with a deformed shape were added to improve the deformation characteristics of concrete. PP fibers were thoroughly scattered to provide an even distribution in the mix. Polypropylene fibers with a deformed shape were used to improve the polymer-concrete bond, because the mechanical bond of ordinary polypropylene fiber with the cement matrix is relatively weak. The properties of PP fibers are given in Table 4.

Table 4. Characteristics of fibers.

Properties	Value	
	Ordinary Polypropylene (PP) Microfiber	Polypropylene (PP) Macrofiber with Deformed Shape
Fiber length	12 mm	45 mm
Shape of the cross-section	Round ( $\varnothing$ 18 ÷ 20 $\mu$ m)	Rectangular (1.0 × 0.5 mm)
Aspect ratio	630	56
Type/form	Micro/monofilament	Macro/monofilament
Specific weight	0.91 g/cm <sup>3</sup>	0.91 g/cm <sup>3</sup>
Melting point	162 °C	164 °C
Flash point	593 °C	>550 °C

A general view of fibers with deformed shape and microfibers can be seen in Figures 2a and 2b, respectively.

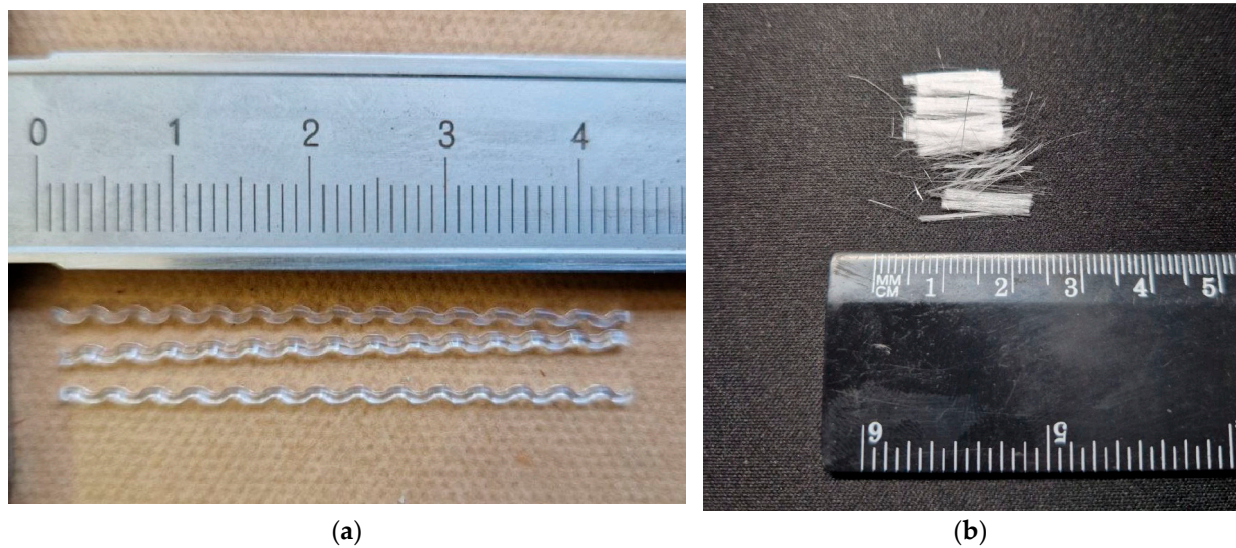


**Figure 2.** Polypropylene fibers used in the study: (a) fibers with deformed shape; (b) microfibers.

The morphology of the investigated materials was examined with the scanning electron microscope SEM FEI Quanta 250 FEG, equipped with EDS. Five mix-proportions were designed, reference mix R and four mixes (R0, R, R+F, R+F+A, R+Z+F+A) containing mineral additions and chemical admixtures. They were designed according to [39], and the compressive strength of concrete was tested according to [40]. The mix-proportions are presented in Table 5.

**Table 5.** The mixture proportions (W/C = 0.36, slump class of fresh concrete—S4).

Mix Identification	R0	R	R+F	R+F+A	R+Z+F+A
Cement, kg/m <sup>3</sup>	450	450	450	450	405
Zeolitic tuff, kg/m <sup>3</sup>	-	-	-	-	45
Sand, kg/m <sup>3</sup>	400	400	400	300	300
Crushed granite sand (0.63–2 mm), kg/m <sup>3</sup>	-	100	100	100	100
Granite gravel (5.0–10 mm), kg/m <sup>3</sup>	400	370	370	370	370
Granite gravel (10.0–20 mm), kg/m <sup>3</sup>	1000	930	930	930	930
Superplasticizer, % by mass	0.8	0.8	1.5	1.2	1.5
Air-entraining admixture, % by mass	-	-	-	0.4	0.4
Fiber with deformed shape, kg/m <sup>3</sup>	-	-	8	8	8
Ordinary microfiber, kg/m <sup>3</sup>	-	-	1.05	1.05	1.05
The volume of the entrained air, %	1.5	1.5	2.0	6.0	6.0

Samples have been tested according to a three-point bend scheme using a 200 ton hydraulic press, equipped with a power distribution ring as well as load sensor (strain gauge) and deflection gauge [41]. A general view of the test device is given in Figure 3a.

Samples (100 × 100 × 400 mm) with an initial notch of 40 mm in depth and 2 mm in width have been used for testing. Two cycles of loading (up to 10% of the expected peak load) and unloading have been held before testing. Specimens have been loaded continuously until their fracture. Load–deflection curves were recorded using a computer-aided data acquisition system (Figure 3b). An estimate of the fracture energy was obtained from the L–d curves according to the RILEM method (work-of-fracture). All series consisted of four specimens. Cube specimens measuring 100 × 100 × 100 mm were used to determine the compressive strength. Specimens have been molded according to [40] and cured (temperature of 20 ± 2 °C and relative humidity of 95%) for 28 days. Then, specimens were taken out from the curing tanks, and a central notch for samples (100 × 100 × 400 mm) was made using a diamond saw.

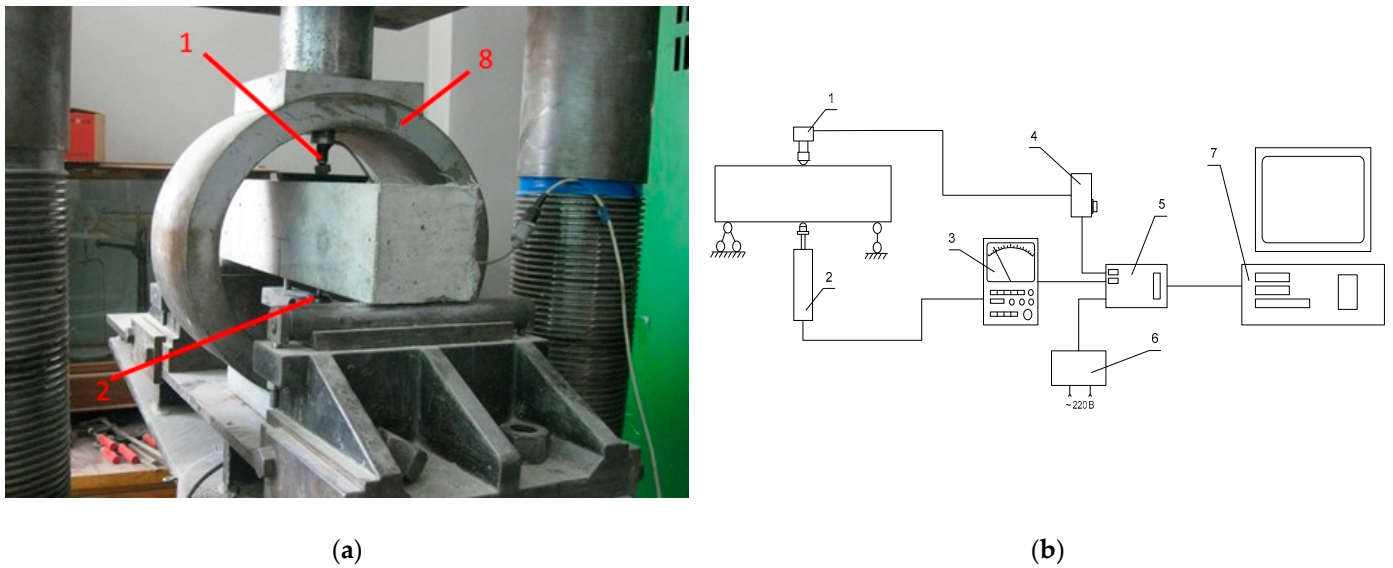


**Figure 3.** (a) General view of test apparatus and (b) scheme of measuring device: 1—strain gauge, 2—deflection gauge, 3—signal amplifier, 4—resistor bridge, 5—interface board, 6—power supply, 7—PC, 8—power distribution ring.

Load–deflection curves were plotted based on the obtained results of the specimens’ tests. The physical and mechanical characteristics of the concrete and the energy characteristics of the fracture were calculated.

### 3. Results and Discussion

It is well known that the brittle behavior of concrete fracture increases with the growth of its compressive strength [27,28]. The properties of concrete with an increased compressive strength, obtained by optimizing technological factors on the different structural levels, were studied. The compressive strength of the designed concrete is shown in Figure 4.

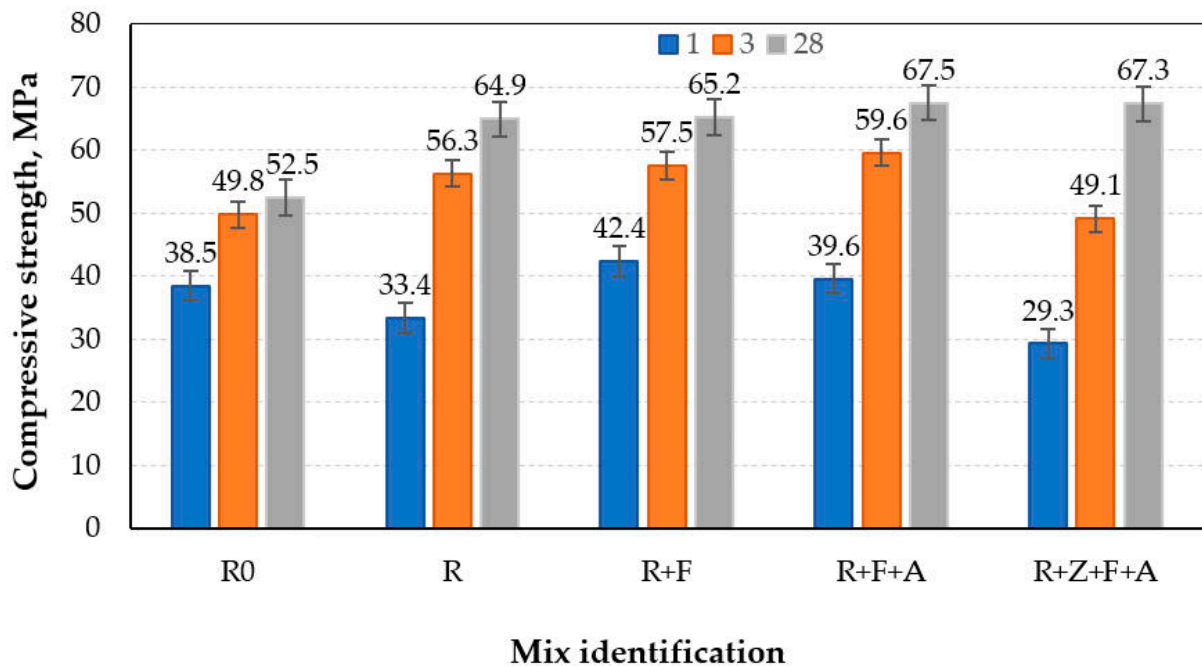


**Figure 4.** The effect of different technological factors on compressive strength of concrete.

As can be seen from the obtained results, the optimization of the concrete grain size results in the reduction of the compressive strength of reference concrete R by 13.3% after 1 day of hardening in comparison with concrete denoted R0. The more intensive kinetics of the strength development of concrete R are observed with the further hardening of such concrete. Thus, the strength of concrete R increases by 23.6% after 28 days. Following the optimization of various types of fibers [33], the appropriate dosages were incorporated into the reference concrete. The results show that concrete's compressive strength increases slightly compared to concrete R. Smarzewski [42] states that polypropylene fibers do not have a significant effect on the compressive strength of high-performance self-compacting concrete after 28 days of hardening because added fibers adversely affect the workability of fresh concrete and, as a result, voids can be created in the concrete, reducing a possible strength increase. Some growth of compressive strength is observed due to the retardation of matrix fracturing because PP fibers limit crack propagation. Broda [43] also showed that a slight influence on the compressive strength was observed when fibers with a length of 5 mm, 10 mm and 15 mm in quantities of 0.25%, 0.75%, and 1% were used in the mixture. Grabiec et al. [44] studied the influence of different dosages (2 and 4%) of polypropylene fibers with a length of 48 mm on the compressive strength of concrete and revealed a positive effect. The concrete incorporating air-entraining agent R+F+A is characterized by a 6.6% lower early strength and a 3.7 and 3.5% higher strength after 3 and 28 days, respectively. The use of an optimal amount of zeolitic tuff [13,45] causes a slight decrease of 12.3 and 12.8% of the early strength of concrete R+Z+F+A compared to the reference concrete R after 1 and 3 days of hardening, respectively, and a 3.7% higher compressive strength after 28 days of hardening.

It should be noted that concrete with such an increased strength is characterized by more brittle behavior compared to conventional concrete. As shown in Figure 5, the behavior of concretes, except concrete R+Z+F+A, do not differ significantly in the elastic stage, which the linear ascending branches of the load–deflection curves indicate. A more inclined ascending branch of the load–deflection curve in the pre-peak stage demonstrates the increase of the fracture toughness of R+Z+F+A concrete. A similar behavior is observed in the post-cracking stage for concretes R0 and R. The results show that this concrete exhibits a consistent behavior throughout all stages of deformation under load. A significant difference is visible in the post-cracking stage for other concretes. The descending part of the load–deflection curve is rather steep for all concrete series. The tail of the descending branch is short for concretes R and R0. The use of an optimal amount of both increases the volume under the descending branch tail significantly. This indicates that the toughness of the concrete increases in comparison with R0 despite the higher compressive strength class. Rao and Prasad [28] reported that the tail of the descending branch would be longer in the case of conventional concretes and shorter in HSC. Adding an air-entraining agent makes the tail smaller. After the partial replacement of Portland cement in concrete R+F+A with zeolitic tuff (10% by mass), the fracture behavior of such concrete under load is similar to concrete R+F. However, this concrete will have a better resistance to freezing and thawing cycles and, as a result, a durability that conforms to a sustainable development strategy [13].

The area under the complete load–deflection curve (Figure 5) represents the total fracture energy  $G_F$ . Figure 6 shows the fracture-energy magnitudes of concretes. The obtained results indicate that the fracture-energy difference between concrete R0 and R is negligible. The fracture energy of concrete incorporating different types of fibers has the highest value, reaching 441 N/m. The addition of an air-entraining agent causes a reduction of fracture energy by 32.9%. The fracture energy of concrete denoted R+Z+F+A increases by 35.1% compared to the reference concrete R. This underlines the positive effect of the optimization of technological factors when a concrete mix is designed to provide appropriate fracture parameters and freeze–thaw resistance.

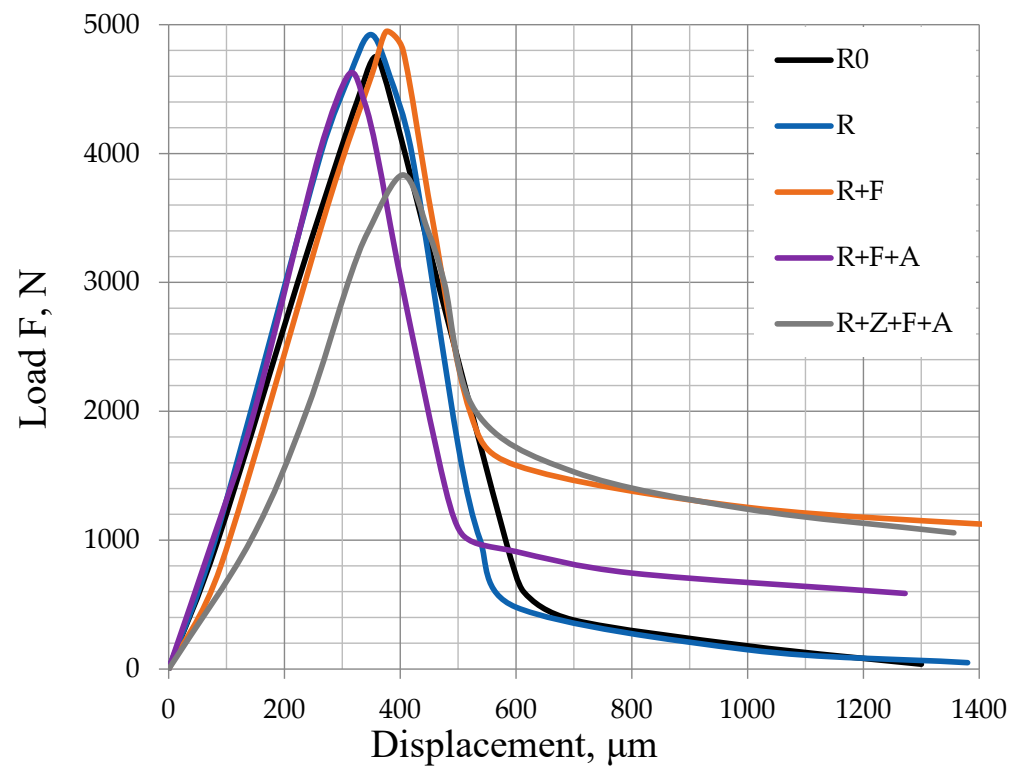


Figure 5. Typical load–deflection curves for studied concretes.

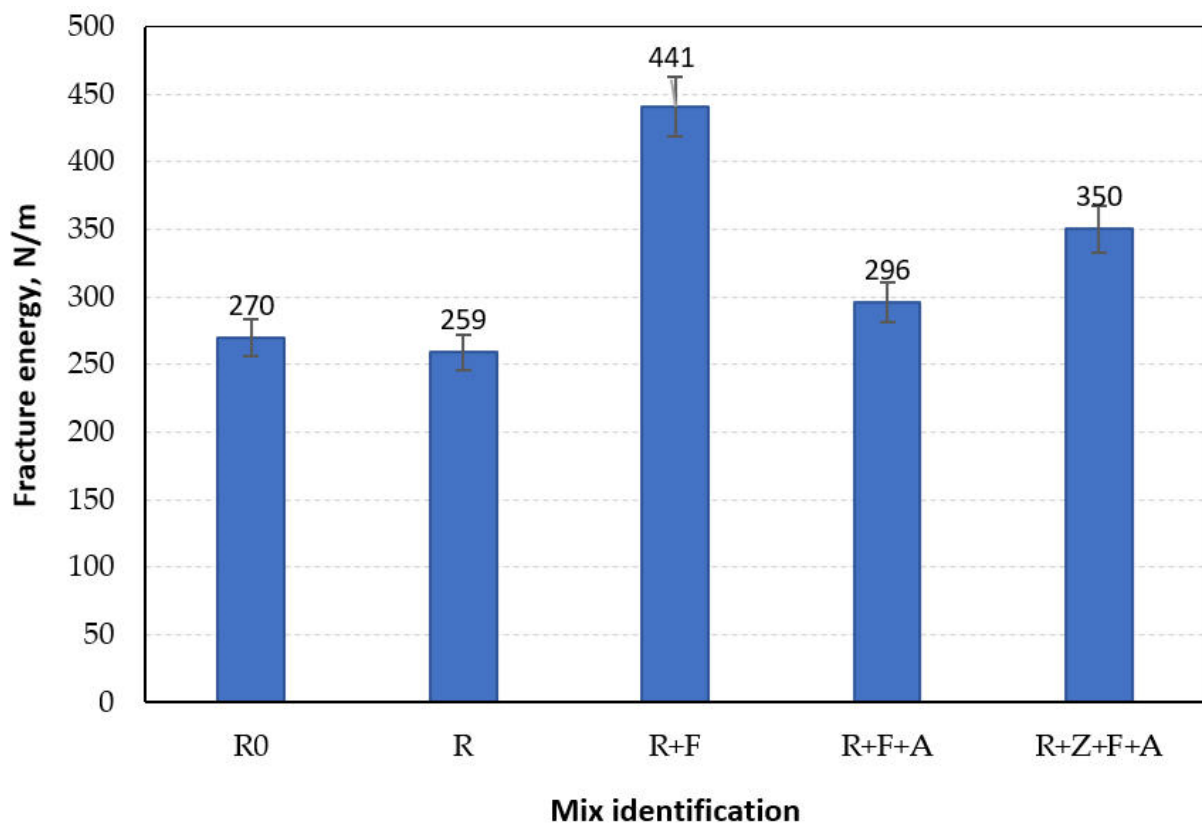
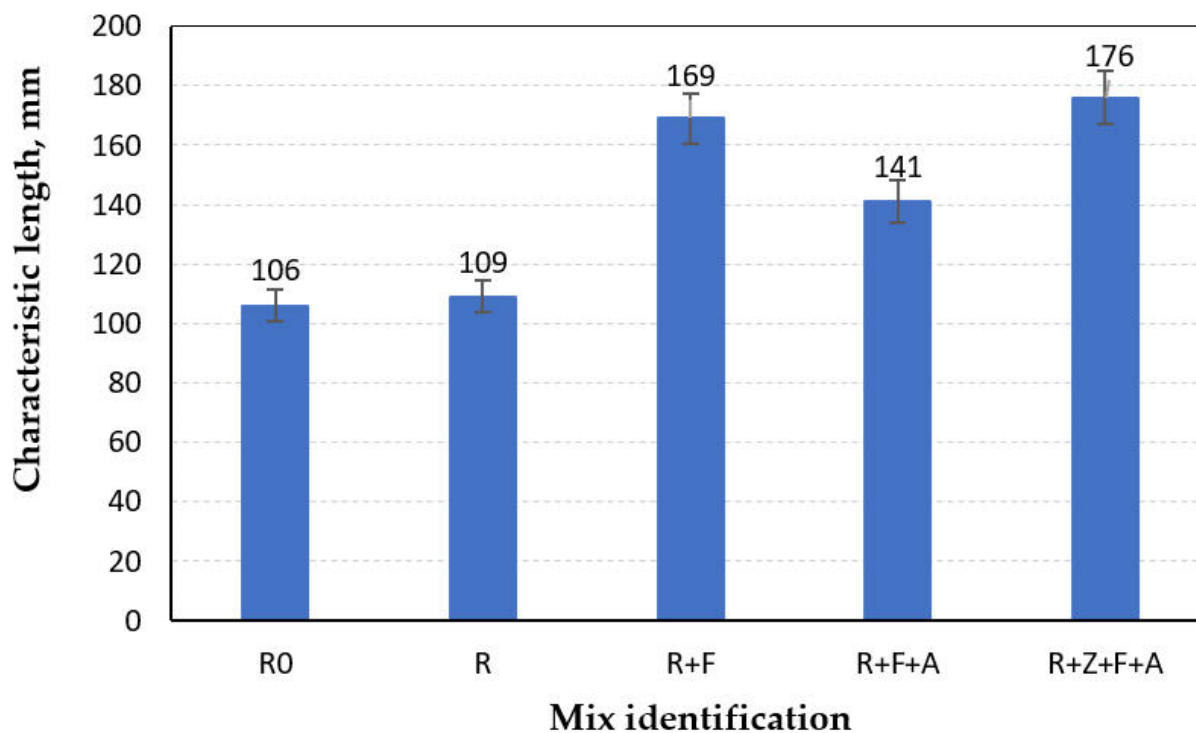


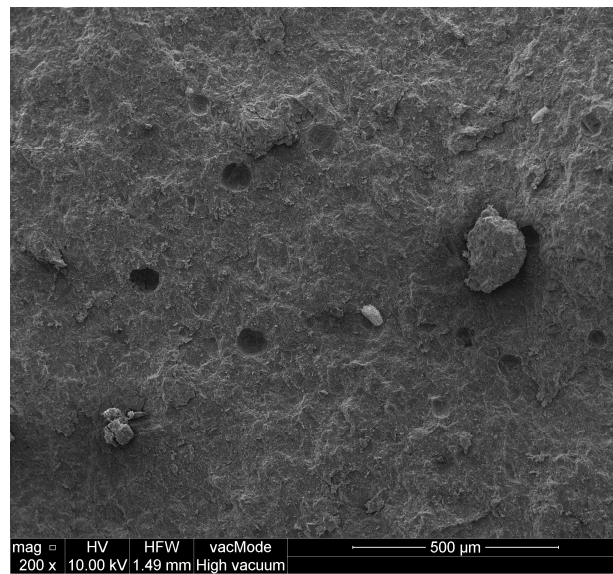
Figure 6. Fracture energy of concretes.

A similar trend can be observed for the characteristic length of studied concretes. Figure 7 reveals that when PP fibers are added to the concrete mix, the characteristic length of concrete R+F increases by 55.0% compared to R. Entrained air bubbles in R+F+A series are flaws in the cement matrix, increasing concrete brittle behavior. This results in a 19.9% lower characteristic length for such a composite. However, the complex addition of zeolitic tuff and air-entraining agent to concrete incorporating different types of fibers improves the characteristic length, which reaches 176 mm and is the highest among tested concretes.

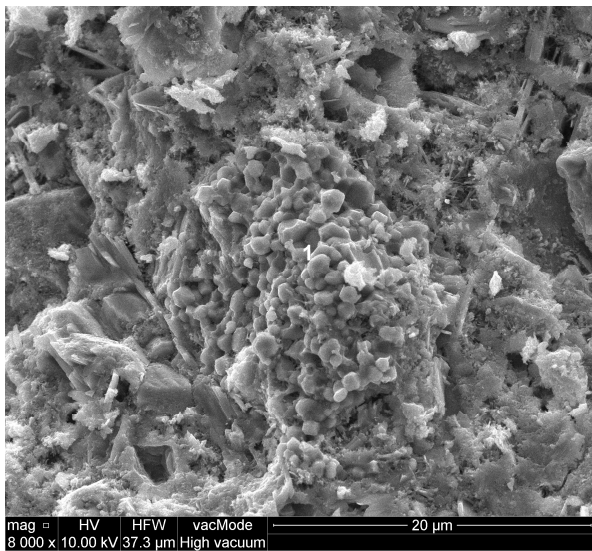


**Figure 7.** Characteristic length of concretes.

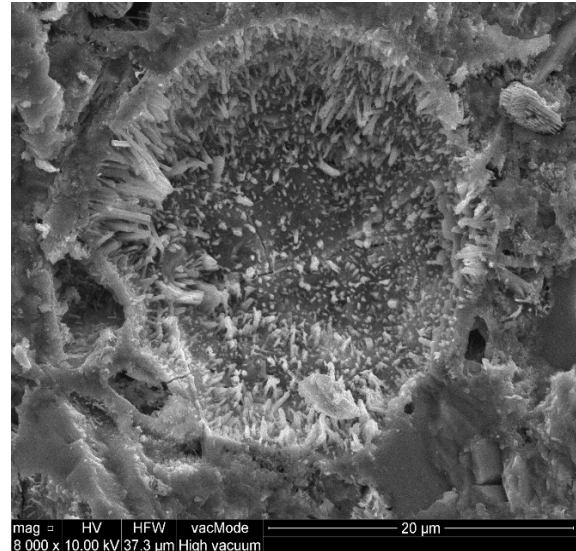
The use of a scanning electron microscope equipped with EDS explains the improvement of the mechanical properties and fracture parameters of concrete incorporating zeolitic tuff and air-entraining agent. Despite its crystalline structure, the zeolitic tuff, which is a hydrated alumina-silicate by nature, shows proper pozzolanic activity. The microstructure of the above-mentioned concrete is characterized by an increased homogeneity (Figure 8b) and the formation of tight submicroscopic clusters of hydrosilicates and calcium hydrosulfoaluminates (Figure 8d). Such concrete also has a structure with an evenly distributed, dispersed air bubble system (Figure 8a). Using a surface active agent as an air-entraining admixture, which consists in most cases of amphiphilic molecules, induces the adsorption of fine cement particles at the air/paste interface, and a particle-armored bubble shell is formed (Figure 8c). The shell's composition depends on the type of cement and used mineral additions. As can be seen from Figure 8e, due to the use of zeolitic tuff, the low-base calcium hydrosilicates in the non-clinker part of the cement matrix of concrete form a tight and robust bubble shell, which in combination with the modified microstructure of concrete results in the enhancement of the mechanical and fracture parameters of concrete. Tunstall et al. [26] confirm the formation of the shell and indicate that the bubble shell improves strength and stability, reducing coalescence.



(a)

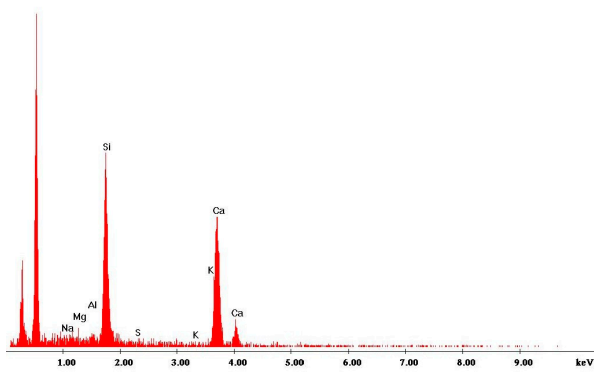


(b)



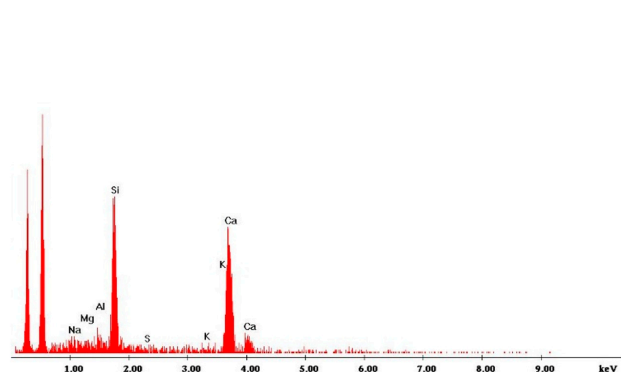
(c)

Label A: Chlorite (Nrm.%= 38.86, 20.96, 34.83, 1.14, 3.84, 0.28)



(d)

Label A: Chlorite (Nrm.%= 38.86, 20.96, 34.83, 1.14, 3.84, 0.28)



(e)

Figure 8. (a–c) Microstructure and (d,e) EDS spectra of concrete cement matrix.

That is why when a load is applied to the air-entrained FRC containing zeolitic tuff, stresses distribute uniformly around the evenly scattered armored bubble shell. This results in an improvement in the compressive strength and fracture parameters of the designed concrete.

#### 4. Conclusions

This article studied the effect of different technological factors on the compressive strength and fracture parameters of concrete with increased strength. A previously optimized amount of zeolitic tuff, different types of fibers and air-entraining agent were used to improve the behavior of concrete under load. The following conclusions can be drawn from the results obtained in the study:

- The compressive strength of concrete increases by 27% after 1 day of hardening when different types of polypropylene fibers are added to concrete. The partial replacement (10% by mass) of Portland cement with zeolitic tuff and the addition of air-entraining agent result in the reduction of early strength, but over time, after 28 days of hardening, the strength of concretes R+F+A and R+Z+F+A is even greater than the strength of concrete R+F by 3.5 and 3.2%, respectively.
- Using zeolitic tuff results in the formation of a tight microstructure and particle-armored bubble shell in the concrete with an air-entraining agent. Low-base calcium hydrosilicates strengthen this shell and are formed in the non-clinker part of the cement matrix due to the excellent pozzolanic activity of zeolitic tuff.
- The concrete incorporating zeolitic tuff, different types of fibers, and an air-entraining agent, despite having a lower Portland cement content (by 10% by mass), exhibits enhanced mechanical properties and fracture parameters, with a 35.1% increase in fracture energy and a 61.5% increase in characteristic length, compared to the reference concrete. This improvement in concrete incorporating an air-entraining admixture is attributed to the even distribution of stresses around the armored bubble shell when the concrete is loaded.
- Both concrete R+F and concrete incorporating an optimized amount of zeolitic tuff, different types of polypropylene fibers, and air-entraining agent R+Z+F+A behave similarly under load in the post-cracking stage. This confirms the efficiency of the proper selection and the optimization of different technological factors, which allow one to obtain economically effective high-quality concrete incorporating a lower cement content. However, a comprehensive life-cycle assessment should be conducted to evaluate the sustainability of the developed concrete.

**Author Contributions:** Conceptualization, T.M. and Y.B.; methodology, Z.B., T.M. and J.S.; validation, Z.B., Y.B. and J.S.; formal analysis, Z.B., T.M. and J.S.; investigation, Z.B., T.M., Y.T., O.H. and J.S.; supervision, T.M., Y.T., Y.B. and O.H.; writing—original draft preparation, Z.B., T.M., Y.T., O.H., Y.B. and J.S.; writing—review and editing, T.M., Y.T., O.H. and J.S.; visualization, O.H., Y.T. and Y.B. All authors have read and agreed to the published version of the manuscript.

**Funding:** This research received no external funding.

**Institutional Review Board Statement:** Not applicable.

**Informed Consent Statement:** Not applicable.

**Data Availability Statement:** The data presented in this study are available on request from the corresponding author.

**Conflicts of Interest:** The authors declare no conflict of interest.

#### References

1. Tomporowski, D.; Markiv, T. Analysis of environmental consequences occurring in the life cycle of a retail facility. *Bud. Archit.* **2022**, *21*, 5–12. [[CrossRef](#)]
2. Ghafari, E.; Feys, D.; Khayat, K. Feasibility of using natural SCMs in concrete for infrastructure applications. *Constr. Build. Mater.* **2016**, *127*, 724–732. [[CrossRef](#)]

3. Kobaka, J.; Katzer, J. A principal component analysis in concrete design. *Constr. Optim. Energy Potential CoOEP* **2022**, *11*, 203–214. [[CrossRef](#)]
4. Jura, J.; Ulewicz, M. Assessment of the Possibility of Using Fly Ash from Biomass Combustion for Concrete. *Materials* **2021**, *14*, 6708. [[CrossRef](#)]
5. Madhuri, P.V.; Kameswara Rao, B.; Chaitanya, A. Improved performance of concrete incorporated with natural zeolite powder as supplementary cementitious material. *Mater. Today Proc.* **2021**, *47*, 5369–5378. [[CrossRef](#)]
6. Ghafari, E.; Ghahari, S.; Feys, D.; Khayat, K.; Baig, A.; Ferron, R. Admixture compatibility with natural supplementary cementitious materials. *Cem. Concr. Compos.* **2020**, *112*, 103683. [[CrossRef](#)]
7. Nagrockiene, D.; Girskas, G. Research into the properties of concrete modified with natural zeolite addition. *Constr. Build. Mater.* **2016**, *113*, 964–969. [[CrossRef](#)]
8. Rovnaníková, P.; Schmid, P.; Keršner, Z. Effect of cement replacement by zeolite on the basic mechanical fracture properties of concrete: A parametric study. *Adv. Mat. Res.* **2014**, *969*, 140–143. [[CrossRef](#)]
9. Małolepszy, J.; Grabowska, E. Sulphate attack resistance of cement with zeolite additive. *Procedia Eng.* **2015**, *108*, 170–176. [[CrossRef](#)]
10. Trník, A.; Scheinherrová, L.; Medved, I.; Černý, R. Simultaneous DSC and TG analysis of high-performance concrete containing natural zeolite as a supplementary cementitious material. *J. Therm. Anal. Calorim.* **2015**, *121*, 67–73. [[CrossRef](#)]
11. Nas, M.; Kurbetci, S. Mechanical, durability and microstructure properties of concrete containing natural zeolite. *Comput. Concr.* **2018**, *22*, 449–459. [[CrossRef](#)]
12. Samimi, K.; Kamali-Bernard, S.; Maghsoudi, A.A.; Maghsoudi, M.; Siad, H. Influence of pumice and zeolite on compressive strength, transport properties and resistance to chloride penetration of high strength self-compacting concretes. *Constr. Build. Mater.* **2017**, *151*, 292–311. [[CrossRef](#)]
13. Markiv, T.; Sobol, K.; Franus, M.; Franus, W. Mechanical and durability properties of concretes incorporating natural zeolite. *Arch. Civ. Mech. Eng.* **2016**, *16*, 554–562. [[CrossRef](#)]
14. Markiv, T.; Sobol, K.; Petrovska, N.; Hunyak, O. The Effect of Porous Pozzolanic Polydisperse Mineral Components on Properties of Concrete. In *Proceedings of CEE 2019; Lecture Notes in Civil Engineering*; Blikharsky, Z., Koszelnik, P., Mesaros, P., Eds.; Springer: Cham, Switzerland, 2020; Volume 47, pp. 275–282. [[CrossRef](#)]
15. Adamczak -Bugno, A.; Lipiec, S.; Vavruš, M.; Koteš, P. Non-Destructive Methods and Numerical Analysis Used for Monitoring and Analyzing Fibre Concrete Deformations. *Materials* **2022**, *15*, 7268. [[CrossRef](#)]
16. Blikharsky, Y.; Selejda, J.; Bobalo, T.; Khmil, R.; Volynets, M. Influence of the percentage of reinforcement by unstressed rebar on the deformability of pre-stressed RC beams. *Prod. Eng. Arch.* **2021**, *27*, 212–216. [[CrossRef](#)]
17. Helbrych, P. Effect of dosing with propylene fibers on the mechanical properties of concretes. *Constr. Optim. Energy Potential CoOEP* **2021**, *10*, 39–44. [[CrossRef](#)]
18. Lipiński, T. Investigation of corrosion rate of X55CrMo14 stainless steel at 65% nitrate acid at 348 K. *Prod. Eng. Arch.* **2021**, *27*, 108–111. [[CrossRef](#)]
19. Lipiński, T.; Wach, A. Influence of inclusions on bending fatigue strength coefficient the medium carbon steel melted in an electric furnace. *Prod. Eng. Arch.* **2020**, *26*, 88–91. [[CrossRef](#)]
20. Pawłowicz, J.A. Computer-aided design in the construction industry—BIM technology as a modern design tool. *Constr. Optim. Energy Potential CoOEP* **2020**, *9*, 89–96. [[CrossRef](#)]
21. Ulewicz, R.; Kleszcz, D.; Ulewicz, M. Implementation of Lean Instruments in Ceramics Industries. *Manag. Syst. Prod. Eng.* **2021**, *29*, 203–207. [[CrossRef](#)]
22. Nagrockiene, D.; Girskas, G.; Skripkiunas, G. Cement freezing-thawing resistance of hardened cement paste with synthetic zeolite. *Constr. Build. Mater.* **2014**, *66*, 45–52. [[CrossRef](#)]
23. Zheng, X.; Zhang, J.; Ding, X.; Chu, H.; Zhang, J. Frost resistance of internal curing concrete with calcined natural zeolite particles. *Constr. Build. Mater.* **2021**, *288*, 123062. [[CrossRef](#)]
24. Pleau, R.; Pigeon, M.; Laurecot, J.L. Some findings on the usefulness of image analysis for determining the characteristics of the air-void system on hardened concrete. *Cem. Concr. Compos.* **2001**, *23*, 237–246. [[CrossRef](#)]
25. Xie, J.; Cui, X.; Guo, N.; Liu, G. Influence of mix proportions on rheological properties, air content of wet shotcrete—A case study. *Appl. Sci.* **2021**, *11*, 3550. [[CrossRef](#)]
26. Tunstall, L.E.; Ley, M.T.; Scherer, G.W. Air entraining admixtures: Mechanisms, evaluations, and interactions. *Cem. Concr. Res.* **2021**, *150*, 106557. [[CrossRef](#)]
27. Einsfeld, R.A.; Velasco, M.S.L. Fracture parameters for high-performance concrete. *Cem. Concr. Res.* **2006**, *36*, 576–583. [[CrossRef](#)]
28. Rao, G.A.; Prasad, B.K.R. Fracture energy and softening behavior of high-strength concrete. *Cem. Concr. Res.* **2002**, *32*, 247–252. [[CrossRef](#)]
29. Solodkyy, S.; Markiv, T.; Sobol, K.; Hunyak, O. Fracture properties of high-strength concrete obtained by direct modification of structure. *MATEC Web Conf.* **2017**, *116*, 01016. [[CrossRef](#)]
30. Zollo, R.F. Fiber-reinforced concrete: An overview after 30 years of development. *Cem. Concr. Compos.* **1997**, *19*, 107–122. [[CrossRef](#)]

31. Emamjomeh, H.; Behfarnia, K.; Raji, A.; Almohammad-albakkar, M. Influence of PVA and PP fibers addition on the durability and mechanical properties of engineered cementitious composites blended with silica fume and zeolite. *Res. Eng. Struct. Mater.* **2023**, *9*, 457–473. [[CrossRef](#)]
32. Zaroudi, M.; Madandoust, R.; Aghaei, K. Fresh and hardened properties of an eco-friendly fiber reinforced self-consolidated concrete composed of polyolefin fiber and natural zeolite. *Constr. Build. Mater.* **2020**, *241*, 118064. [[CrossRef](#)]
33. Turba, Y.; Solodkyy, S.; Markiv, T. Strength and Fracture Toughness of Cement Concrete, Dispersedly Reinforced by Combination of Polypropylene Fibers of Two Types. In *Proceedings of CEE 2019; Lecture Notes in Civil Engineering*; Blikharsky, Z., Koszelnik, P., Mesaros, P., Eds.; Springer: Cham, Switzerland, 2020; Volume 47, pp. 488–494. [[CrossRef](#)]
34. *DSTU B V 2.7-185:2009; Building Materials. Cements. Methods of Determination of Normal Thickness, Setting Time and Soundness.* Ukrarkhbudinform: Kyiv, Ukraine, 2009.
35. *DSTU B V 2.7-187:2009; Building Materials. Cements. Methods of Determination of Bending and Compression Strength.* Ukrarkhbudinform: Kyiv, Ukraine, 2009.
36. *DSTU B V 2.7-188:2009; Building Materials. Cements. Methods of Determination of Fineness.* Ukrarkhbudinform: Kyiv, Ukraine, 2009.
37. *DSTU B V 2.7-232:2010; Building Materials. Sand for Construction Work Testing Methods.* Ukrarkhbudinform: Kyiv, Ukraine, 2010.
38. *DSTU B V.2.7-71-98; Building Materials. Mountainous Rock Road Metal and Gravel, Industrial Waste Products for Construction Works. Methods of Physical and Mechanical Tests.* Kyiv, Ukraine, 1998.
39. *DSTU-N B V.2.7-299:2013; Guidelines for Determining the Composition of Concrete.* Ukrarkhbudinform: Kyiv, Ukraine, 2013.
40. *DSTU B V.2.7-214:2009; Building Materials Concretes Methods for Strength Determination Using Reference Specimens.* Kyiv, Ukraine, 2009.
41. *DSTU B V.2.7-227:2009; Building Materials. Concretes. Methods for Determination of Fracture Toughness Characteristics.* Kyiv, Ukraine, 2010.
42. Smarzewski, P. Fresh and Mechanical Properties of High-Performance Self-Compacting Concrete Containing Ground Granulated Blast Furnace Slag and Polypropylene Fibres. *Appl. Sci.* **2023**, *13*, 1975. [[CrossRef](#)]
43. Broda, J. Application of Polypropylene Fibrillated Fibres for Reinforcement of Concrete and Cement Mortars. In *High Performance Concrete Technology and Applications*; IntechOpen: London, UK, 2016; pp. 189–204.
44. Grabiec, A.M.; Grabiec-Mizera, T.; Slowek, G. Contribution to the knowledge on influence of polypropylene fibres on selected properties of self-compacting concrete. *Architectura* **2014**, *13*, 5–18.
45. Markiv, T.; Huniak, O.; Sobol, K. Optimization of Concrete Composition with Addition of Zeolitic Tuff. *Bull. Lviv Polytech. Natl. Univ. Theory Pract. Constr.* **2014**, *781*, 116–120.

**Disclaimer/Publisher's Note:** The statements, opinions and data contained in all publications are solely those of the individual author(s) and contributor(s) and not of MDPI and/or the editor(s). MDPI and/or the editor(s) disclaim responsibility for any injury to people or property resulting from any ideas, methods, instructions or products referred to in the content.